Targeting aleurone cells for enhanced protein recovery from wheat bran: Impact on protein functionality and phytate content

Journal of Cereal Science 124 (2025) 104205

Contents lists available at ScienceDirect

Journal of Cereal Science

journal homepage: www.elsevier.com/locate/jcs

Targeting aleurone cells for enhanced protein recovery from wheat bran: Impact on protein functionality and phytate content

Helga Gudny Eliasdottir [a,*], Precious Elue Ebube [a], Annika Krona [b], E.R. Kanishka B. Wijayarathna [c], Akram Zamani [c], Mehdi Abdollahi [a,**]

[a] Department of Life Sciences, Food and Nutrition Science, Chalmers University of Technology, SE-41296, Gothenburg, Sweden
[b] RISE Research Institutes of Sweden, Agriculture and Food, Box 5401, 402 29, Gothenburg, Sweden
[c] Swedish Centre for Resource Recovery, University of Borås, Borås, 50190, Sweden

ARTICLE INFO

Keywords:
Wheat bran
Plant-based protein
Side streams
Phytic acid
pH-shift method

ABSTRACT

Protein extraction from wheat bran is challenging due to its multi-layer and fiber-rich structure. Here, opening aleurone cells, via dry and wet milling, their combination and a novel ultrafine milling, and its effect on wheat bran's protein recovery using the alkaline solubilization/isoelectric precipitation and protein structure, functionality, and phytate content were investigated. Wet milling and ultrafine milling improved protein recovery and purity but only ultrafine milling reduced bran particle size to the aleurone cells and exposed their structure. Despite this, ultrafine milling did not significantly increase protein yield compared to wet milling, which partially opened the aleurone cells, meaning that opening the cells per se is not enough for extracting their protein. Proteins extracted with the aid of ultrafine milling had smaller particle sizes with significantly better water solubility (>2-fold) and rheological properties. Both wet milling and ultrafine milling significantly improved the removal of phytate during the wet fractionation process. Altogether, optimizing milling techniques offers a promising path to enhance accessibility to wheat bran proteins and their quality if carefully fine-tuned but other assistant technologies are necessary for boosting the recovery of the released protein from aleurone cells.

1. Introduction

A shift in food consumption and production towards plant-based resources is urgently needed to reduce the environmental burden of the food system while meeting the growing global protein demand. However, the plant-based food sector faces the challenge of inefficiency along its production value chains leading to significant amounts of side stream and waste. The use of plant-based side streams is further complicated by issues such as suboptimal nutrient composition and complicated structures of the side streams, the presence of anti-nutrients and off-flavor compounds (Oreopoulou and Tzia, 2007).

Wheat bran (WB) accounts for 15–20 % of wheat seed weight and is the main side-stream of the wheat milling industry. Its global annual production is estimated at approximately 150 million tons (Chen et al., 2023). Considering its high nutritional value—being rich in dietary fibers (40–50 %), proteins (14–20 %), phenolic compounds, minerals, and vitamins—wheat bran (WB) has been widely investigated for direct use in food (Chen et al., 2023). However, due to its complex structure and composition that negatively affect sensory attributes, over 90 % of globally produced WB is still used for animal feed (Onipe et al., 2017). Therefore, valorising WB, particularly as a protein source, presents a promising opportunity to enhance its food applications and to address the growing demand for plant-based proteins.

One of the most common methods used for protein extraction from plant-based biomasses is alkaline solubilization followed by isoelectric precipitation or the so-called pH-shift process. In this method, proteins in the biomass are solubilized in water at alkaline pH, enabling their separation from fibers via centrifugation. The proteins are then aggregated by lowering the pH to their isoelectric point and dewatered through centrifugation or filtration. This method is highly efficient for extracting proteins from legumes like soy and pea, which contain over 70 % easily accessible alkali-soluble globulins, primarily surrounded by starch globules. However, applying the classic pH-shift method to cereal side streams, particularly WB, is challenging and often yields low

* Corresponding author.
** Corresponding author.
E-mail address: khozaghi@chalmers.se (M. Abdollahi).

https://doi.org/10.1016/j.jcs.2025.104205
Received 23 March 2025; Received in revised form 3 May 2025; Accepted 12 May 2025
Available online 13 May 2025

protein recovery and purity (Janssen et al., 2023). This is due to several factors. First, the fiber-rich, multilayer structure of wheat bran creates physical barriers that hinder protein accessibility and but also solubilization since fibers tightly interact with proteins. Second, wheat bran contains a heterogeneous protein composition, with lower amounts of albumins and globulins (33–39 %) and higher levels of insoluble glutelins and prolamins (11–16 %) (Janssen et al., 2023). To enhance protein extraction efficiency from WB, it is essential to improve protein accessibility by breaking down its physical structure.

WB consists of multiple layers: the outer pericarp, inner pericarp, testa (seed coat), hyaline layer, and aleurone layer (AL). While proteins in the outer and intermediate bran layers are readily extractable, accessing the proteins in the AL is particularly crucial. The AL comprises about 50 % of the WB and accounts for approximately 15 % of the total wheat protein content. Notably, its proteins offer a better amino acid balance than those in the endosperm and contain 30 % of the total lysine (Brouns et al., 2012). Most of the proteins in the AL are found inside the cell contents with over 75 % resembling globulin-like storage proteins with a high nutritional profile (Chen et al., 2023). The challenge is that AL is situated at the innermost part of the WB and consists of very small cells, measuring 37–65 μm by 25–75 μm (Brouns et al., 2012; De Bondt et al., 2020). Several studies have explored both biological and mechanical strategies to break down the WB structure down to the aleurone layer, enhancing the accessibility of its proteins and nutrients for direct use as food ingredients. While enzymatic treatments and fermentations have shown limited success, recent advancements in mechanical methods, particularly ultra-fine milling, have proven to be highly effective. De Bondt et al. (2020) showed that both wet milling via bead miller and cryogenic milling managed to reduce WB particle size down to 28–38 μm which opened all the aleurone cells in the bran. In addition, Li et al. (2023) reported that ultra-fine milling of WB down to 19 μm disrupted aleurone cells which increased its total protein extractability using the Osborne fractionation method but they did not continue with extracting the proteins with the pH-shift method. Previously, De Brier et al. (2015) also reported that ball milling was more effective than enzymatic treatment for releasing proteins from wheat bran (WB) under alkaline conditions at 60 °C; however, they did not continue with the precipitation of these proteins using a complete pH-shift method. To our knowledge, no studies have reported the effects of various fine milling methods and their intensities on protein extraction efficiency from WB using the pH-shift method.

Another crucial consideration is that fine milling may also liberate other compounds, including soluble and insoluble fibers, phenolic compounds, and phytate, which can result in their co-extractability. This co-extraction can hinder protein extraction efficiency during both the extraction and precipitation phases, potentially compromising protein purity, functionality, and nutritional value. Excessive milling may lead to protein degradation or aggregation, negatively impacting protein functionality, necessitating careful investigation (Liu et al., 2021a). However, the effect of fine milling on the techno-functional properties of WB protein remains unknown.

In addition, AL is the main reservoir of phytate in WB, representing more than 87 % of phosphorus content in the wheat kernel. Phytate is a heat-resistant antinutritional compound that can chelate minerals such as iron and zinc and reduce their bioavailability in the human body which is a critical challenge ahead of the plant-based protein industry (Thakur et al., 2019). Phytate can be released by fine milling down to the size of aleurone cells (Chen et al., 2013). Guo et al. (2015) showed that removing the aleurone cells using a roller mill reduced the phytate content of WB by 62 %. Consequently, the impact of fine milling down to a particle size less than the aleurone cells on the recovery or reduction of phytate content in wheat bran protein requires a thorough evaluation, as this remains largely unexplored.

This study aimed to evaluate the effect of dry milling via ball mill (BM), wet milling via high shear mechanical homogenizer (HSMH), their combination and ultrafine grinding via supermass colloider (SC) on protein recovery from WB using alkaline solubilization followed by isoelectric precipitation. The key question was whether opening the aleurone cells via extensive milling will improve protein recovery during the subsequent wet fractionation. The effect of the most efficient milling techniques on zeta-potential, polypeptide pattern, water solubility, emulsification capacity, and rheological properties of the recovered WB proteins was also investigated. The possible effect of fine milling intensity on the phytate content of the recovered proteins was also evaluated.

2. Materials and methods

2.1. Raw materials and chemicals

Commercial WB was produced using an industrial roller mill and supplied by Lantmännen (Lidköping, Sweden). Commercial WB will be called “Industrial mill” (IM) in this publication. The main components of WB are carbohydrates (57.4 %) and protein (14.7 %). The WB was obtained in dry form but had a moisture content of 11.24 %. The composition data for the commercial WB was provided by Lantmännen and was not analyzed in this study again. Sodium hydroxide as pellets, hydrochloric acid, and SDS were reagent grade and purchased from Sigma-Aldrich (Sigma-Aldrich, Germany). All the other used chemicals were analytical grade.

2.2. Mechanical disruption of wheat bran with different milling technologies and intensities

2.2.1. Dry milling with ball mill

A planetary ball mill in laboratory scale (Retsch, MM400, 42,781 Haan, Germany) was used for dry milling of the WB. For this purpose, 4 g of WB was placed into a 50 mL steel jar along with two stainless steel beads with a diameter of 1 cm. To achieve different particle sizes, the sample was subjected to ball milling for 10, 20, and 30 min at a frequency of 30 1/s. The process was repeated five times to produce a total of 20 g WB. The sample temperature was checked after milling to ensure the sample had not experienced heating during the milling process. The mixture was subsequently used for protein extraction as explained in section 2.3.

2.2.2. Wet milling with high-shear mechanical homogenizer

For wet milling, 20 g of WB was added to 300 mL of distilled water (1:15 v/w ratio) and then subjected to milling with a high-shear mechanical homogenizer (HSMH) (LM5, Silverson, MA, US) equipped with a radial discharge head. To achieve different milling levels and particle sizes, the process was tested for both 3 min and 10 min. To avoid overheating the samples were cooled down by putting them into a container with ice cubes and cold water during the milling process. The mixtures were subsequently used for protein extraction as explained in section 2.3.

2.2.3. Ultrafine milling with supermassive colloider

After a series of protests exploring various WB-to-water ratios and milling conditions and time, wet milling with supermass colloider was performed using a suspension of WB in water (250 g WP in 2 L of distilled water). The mixture was passed 49 times through a supermass colloider (SC) (MKCA6-5 J, Masuko Sangyo, Kawaguchi, Japan) with MKE46 grinding stones and a rotor speed of 2700 rpm and with different positive and negative clearances. Initially, the mixture passed twice through a positive clearance of 200 μm and twice through a positive clearance of 100 μm. Then, it was run five times at 0 μm, ten times at −30 μm, ten times at −50 μm, ten times at −70 μm and ten times at −100 μm. The mixture was subsequently used for protein extraction as explained in section 2.3.

2.2.4. A combination of dry and wet milling

To achieve a combination of dry and wet milling, the WB was first subjected to ball milling for 10, 20, and 30 min at a frequency of 30 1/s. Then, each sample was separately mixed with distilled water at a 1:15 v/w ratio and HSMH was performed for 3 or 10 min 10 min of ball milling was referred to as large (L), 20 min as medium (M) and 30 min as small (S) in this experiment.

2.3. Protein extraction using alkaline solubilization followed by isoelectric precipitation

Each milled WB sample was mixed with distilled water in a 1:15 v/w ratio or its ratio was adjusted to 1:15 b y adding extra water, which was needed for the SC sample. Then, the pH of the WB homogenates was adjusted to pH 11.0 using 1.0 N NaOH and incubated under stirring for 1 h using a magnetic stirrer at ambient conditions while the pH remained constant. The suspension was then centrifuged (Sorvall LYNX6000, Thermo Scientific, MA, USA) (5500×*g* for 20 min at 20 °C) and the emerging pellet was separated from the supernatant using a sieve. Then, the pH of the supernatant was lowered to WB isoelectric point of 4.5 (defined by pretests) and incubated under stirring for 10 min using a magnetic stirrer, at ambient conditions. The supernatant was centrifuged (5500×*g* for 20 min at 20 °C). The pellet containing WB protein was then collected, weighed and dried using a freeze-drier.

2.4. Measurement of protein recovery, purity and mass yield

The total nitrogen content was determined using the DUMAS combustion method (elemental analyzer) (Elementar Analysensysteme GmbH, Hanau, Germany) using 2 mg of each recovered WB protein and WB start material. The total nitrogenous content was then converted to protein using 5.4 as a conversion factor (Mariotti et al., 2019). All analysis was performed in triplicate.

The protein purity, mass yield and protein recovery were calculated with the following formulas:

$$\text{Protein purity (\%)} = \text{Nitrogen content (\%) x 5.4} \quad (1)$$

$$\text{Mass yield (\%)} = \frac{\text{Weight of recovered dry WB protein (g)}}{\text{Weight of used starting WB biomass (g)}} \times 100 \quad (2)$$

$$\text{Protein recovery (\%)} = \frac{\text{Weight of WB protein (g)} \times \text{Protein content of WB protein (\%)}}{\text{Weight of used starting WB (g)} \times \text{Protein content of WB (\%)}} \times 100 \quad (3)$$

2.5. Microstructure analysis

To understand the effect of milling on the structure of WB particles and extractability of its proteins during the pH-shift processing, the microstructure of the industrially milled WB, homogenates (H) and the first pellets (P1) of samples subjected to HSMH and SC was analyzed using light microscopy. The wet samples were directly frozen in liquid nitrogen, but the dry samples were dispersed in Milli-Q water and re-wetted for 30 min and then frozen in liquid nitrogen. Samples were cut into 7 μm sections in a Leica CM3050S cryostat and applied to microscopy slides. Cryosections were stained with a mixture of light green and Lugol's solution and examined with an Olympus BX53 light microscope (LM) (Olympus Life Science, Tokyo, Japan). Proteins were stained green and starch was stained blue, but the fibers were detected unstained. Micrographs were captured at different magnifications with a CMos SC50 camera (Olympus Life Science) and processed with the Olympus software cellSense Entry.

2.6. Characterization of recovered wheat bran proteins

2.6.1. Sodium dodecyl sulfate-polyacrylamide gel electrophoresis (SDS-PAGE)

The polypeptide profiles of WB proteins were determined with SDS-PAGE according to the method by Laemmli (1970). First, 1 g of each sample was mixed with 9 mL of 5 % SDS solution and homogenized using Ian KA polytron Ultra-Turrax (T18 basic ULTRA-TURRAX®, IKA, Germany) at 11,000 rpm for 2 min. The homogenate was heated using a water bath (JULABO GmbH, Seelbach, Germany) at 85 °C for 1 h to dissolve the proteins, followed by centrifugation at 20 °C. The protein content of the supernatant was determined using a modified version of the Lowry protein determination method (Markwell et al., 1978). The samples were then diluted using 5 % SDS to reach 4 μg protein/μL, mixed with an equal amount of Laemmli buffer (Bio-Rad, USA) containing 5 % β-mercaptoethanol and heated at 95 °C for 5 min using a heater block (ThermoScientific, MA, USA). After cooling, the samples were centrifuged at 5000×*g* for 5 min. Afterward, 20 μL of each sample was loaded onto the gel (4–20 % Mini-PROTEAN® TGX™ Precast Protein Gels, BioRad) together with 5 μL of a marker representing a broad range (10–250 kDa) of polypeptide bands. The gel was stained using a 0.02 % (w/v) Coomassie Brillian Blue R-250 in 50 % (v/v) methanol and 7.5 % (v/v) acetic acid for 30–60 min. Destaining was performed using 50 % methanol (v/v) and 7.5 % (v/v) acetic acid for 30 min. Quantification of bands was conducted using Bio-Rad Image Lab 6.1.0. software (Bio-Rad Laboratories, Hercules, CA, USA).

2.6.2. Water solubility

The water solubility of the WB proteins at different pH values was measured. Initially, 500 mg of each WB protein was dispersed in 20 mL of distilled water and its pH was adjusted to 3.0–11.0 using 1.0 M NaOH or HCl and kept constant at each pH-value and temperature of 20 °C for 30 min using a magnetic stirrer. Then, the solutions were centrifuged at 15,000×*g* for 30 min at 4 °C and the soluble protein content in the supernatants was determined using the modified Lowry protein determination method using bovine serum albumin as standard (Markwell et al., 1978). The protein solubility of the samples was calculated using the following equation (4):

$$\text{Protein solubility (\%)} = \frac{\textit{Protein concentration in supernatant } \left(\frac{mg}{mL}\right)}{\textit{Protein concentration in pH with maximum solubility } \left(\frac{mg}{mL}\right)} \times 100 \quad (4)$$

2.6.3. Zeta-potential and particle size distribution

Zeta potential (ζ) and particle size readings were conducted with a dynamic light scattering analytical instrument (DLS Zetasizer Ultra, Malvern Panalytical Limited, Worcestershire, UK) according to (C. Li et al., 2023). First, 25 mg of each WB protein was dispersed in 25 mL of distilled water (1.0 mg/mL). The pH of the samples was adjusted to a desired range (3.0–11.0) using 1.0 M NaOH or 1.0 M HCl and incubated at each pH value at ambient conditions for 30 min while mixed using a magnetic stirrer. The samples were then diluted to reach 0.1 $\frac{mg}{mL}$ using distilled water with the same pH and centrifuged at 5500×*g* for 30 min at 4 °C and the supernatant was used for zeta potential measurement. Particle size measurements were conducted for the centrifuged samples at pH 7, after zeta potential measurements using the same instrument. The DLS Zetasizer Ultra, could measure particle sizes between 0.3 nm and 10 μm. Zeta potential and particle size measurements were performed in triplicate.

2.6.4. Emulsification properties

Emulsifying activity index (EAI) and emulsion stability index (ESI) of the proteins were analyzed by creating an oil-in-water emulsion. First, 300 mg of each WB protein was dispersed in 30 mL of distilled water and 10 g of sunflower oil was added to them and homogenized using an Ultra Turrax homogenizer at 20,000 rpm for 1 min. EAI was determined by transferring 50 μL of the emulsion from the bottom of the container to 5 mL of 0.1 % SDS solution and reading its absorbance at 500 nm using a UV–visible spectrophotometer (Cary 60 UV–vis, Agilent technologies, Santa Clara, USA) at room temperature. ESI was evaluated by measuring the absorbance of the emulsion at 500 nm after 10 min. Measurements were performed in duplicates and the EAI and ESI values were calculated based on using the following equation:

$$EAI\left(\frac{m^2}{g}\right) = \frac{2 \times 2.303 \times A_0 \times DF}{C \times \varphi \times \theta \times 10000} \quad (5)$$

$$ESI\ (min) = \frac{A_{10} \times \Delta t}{\Delta A} \quad (6)$$

A_0 is the absorbance at t = 0 min, A_{10} is the absorbance at t = 10 min, *DF* is the dilution factor, *C* is the initial protein concentration (g/mL), φ is the volume fraction of oil in the emulsion, θ is the path length of cuvette (1 cm), Δt is the elapsed time (10 min), ΔA is the absorbance difference between t = 0 and t = 10 min.

2.6.5. Surface color

The surface color of the WB proteins was monitored using a Minolta colorimeter (CR-400, Konica Minolta Sensing, Japan). Each sample was poured into a small Petri dish (5–6 mm), placed on top of the colorimeter and subjected to the measurement with five replicates. Color was measured in the L × a*b (CIELAB) color space.

2.6.6. Rheological properties

To understand heat-induced gelation behavior of the proteins, an *in-situ* gelation was carried out as described by Sajib et al. (2023). For the assay, 3 g of each WB protein was added to 12 mL of milliQ water and mixed using a magnetic stirrer for 30 min. A small portion of the sample (around 1–2 g) was loaded on a dynamic rheometer (Paa Physica Rheometer MCR 300, Anton Paar GmbH, Austria). The rheometer was equipped with a parallel-plate geometry with a plate diameter of 25 mm and a plate gap of 1 mm, and it was operated in an oscillating mode. Mineral oil was added to the edges of the sample and a cover was put on to prevent evaporation. In-situ gelation was performed in four steps; ramping up the temperature from 20 °C to 90 °C at a constant heating rate of 5 °C/min, followed by a constant temperature at 90 °C for 30 min, and then the temperature was ramped down to 20 °C at a rate of 5 °C/min and finally 10 min of conditioning at 20 °C. The gelation test was done in a linear viscoelasticity region (i.e., 1 % strain and 0.1 Hz frequency) of the samples.

An amplitude sweep test was performed, consequently, after the *in-situ* gelation to determine the strength of the gel formed from each protein. The test was performed over a strain range of 0.01–1000 % (ramp logarithmic mode) at a constant frequency of 0.1 Hz and at 20 °C. The yield stress was determined by the crossover point of G′ and G″ for each sample. Measurements for each protein sample were done in duplicates.

2.6.7. Phytate analysis

Phytate was analyzed as inositol hexaphoshate (IP6) by high-performance liquid chromatography (HPLC) according to the method of Carlsson et al. (2001) (Carlsson et al., 2001). For this purpose, 0.5 g of the WB start biomass and the three types of WB protein (IM, 10min HSMH, and SC) were mixed with 10 mL of 0.5 mol/L HCl for 3 h using a laboratory shaker (Heidolph Reax 2; Heidolph Instruments GmbH Schwabach, Germany). Then, 1 mL of each sample was transferred into Eppendorf tubes and centrifuged for 5 min at 12,000×*g*, 20 °C, and then the supernatants were transferred to HPLC vials. A rapid analysis of IP6 (isocratic eluent) was performed at a flow rate of 0.8 mL/min, with 80 % of 1 M HCl and 20 % milliQ H_2O. The injection volume was 50 μL, and the analysis time was 7 min for each sample. The eluents were mixed with 0.1 % $Fe(NO_3)_3$*$9H_2O$ in a 2 % $HClO_4$ solution in a post column reactor. The combined flow rate was 1.2 mL/min. A mixing tee and a homemade reaction coil made of a crocheted Teflon tube (i.d 0.2 mm, 4.5 m) optimized with respect to reaction time and to avoid peak broadening, was applied to get enough reaction time and blending rate. Calculations of peak area, elution times, regression equation and standard curves were done with the software, ChromNav. The phytate concentration was calculated based on an external standard with a concentration range of 0.1–0.6 μmol/mL.

Table 1
Protein recovery, mass yield (in dry weight (dw)), and protein purity of wheat bran subjected to different types of milling and at different intensities. The highlighted results represent the types of milling selected for testing rheological and functional properties. Industrial mill (IM, control), high-shear mechanical homogenization (HSMH), ball milling (BM), supermass colloider (SC).

	Protein recovery (%)	Mass yield (dw) (%)	Protein purity (%)
Industrial mill (IM)	***29.35 ± 0.92^{a}***	***9.35 ± 0.85^{a}***	***46.06 ± 2.03^{a}***
3 min-HSMH	*39.82 ± 2.48^{bcd}*	*10.78 ± 0.04^{abc}*	*54.25 ± 3.21^{b}*
10 min-HSMH	***42.37 ± 0.36^{d}***	***10.76 ± 0.6^{abc}***	***57.91 ± 2.88^{b}***
Small ball mill	*35.48 ± 0.95^{bc}*	*9.48 ± 0.04^{a}*	*54.97 ± 1.30^{b}*
Medium ball mill	*37.96 ± 4.53^{bcd}*	*10.80 ± 1.20^{abc}*	*51.58 ± 0.40^{ab}*
Large ball mill	*34.05 ± 0.47^{ab}*	*9.60 ± 1.27^{ab}*	*52.49 ± 6.20^{ab}*
Small ball mill + 3 min-HSMH	*41.74 ± 0.25^{d}*	*10.70 ± 0.14^{abc}*	*57.28 ± 1.09^{b}*
Medium ball mill + 3 min-HSMH	*42.00 ± 0.47^{d}*	*10.84 ± 0.29^{abc}*	*56.87 ± 0.90^{b}*
Large ball mill + 3 min-HSMH	*41.81 ± 0.31^{d}*	*10.87 ± 0.40^{abc}*	*56.52 ± 1.67^{b}*
Small ball mill + 10 min-HSMH	*40.82 ± 3.18^{cd}*	*11.30 ± 0.07^{c}*	*53.02 ± 3.81^{ab}*
Medium ball mill + 10 min-HSMH	*40.07 ± 4.62^{bcd}*	*11.55 ± 0.07^{c}*	*54.53 ± 1.11^{b}*
Large ball mill + 10 min HSMH	*40.13 ± 1.03^{bcd}*	*11.23 ± 0.46^{bc}*	*52.56 ± 3.49^{ab}*
Supermass colloider	***42.45 ± 4.95^{d}***	***11.18 ± 1.17^{bc}***	***55.74 ± 0.70^{b}***

Data within the same column carrying a different superscript letter are significantly different ($p < 0.05$).

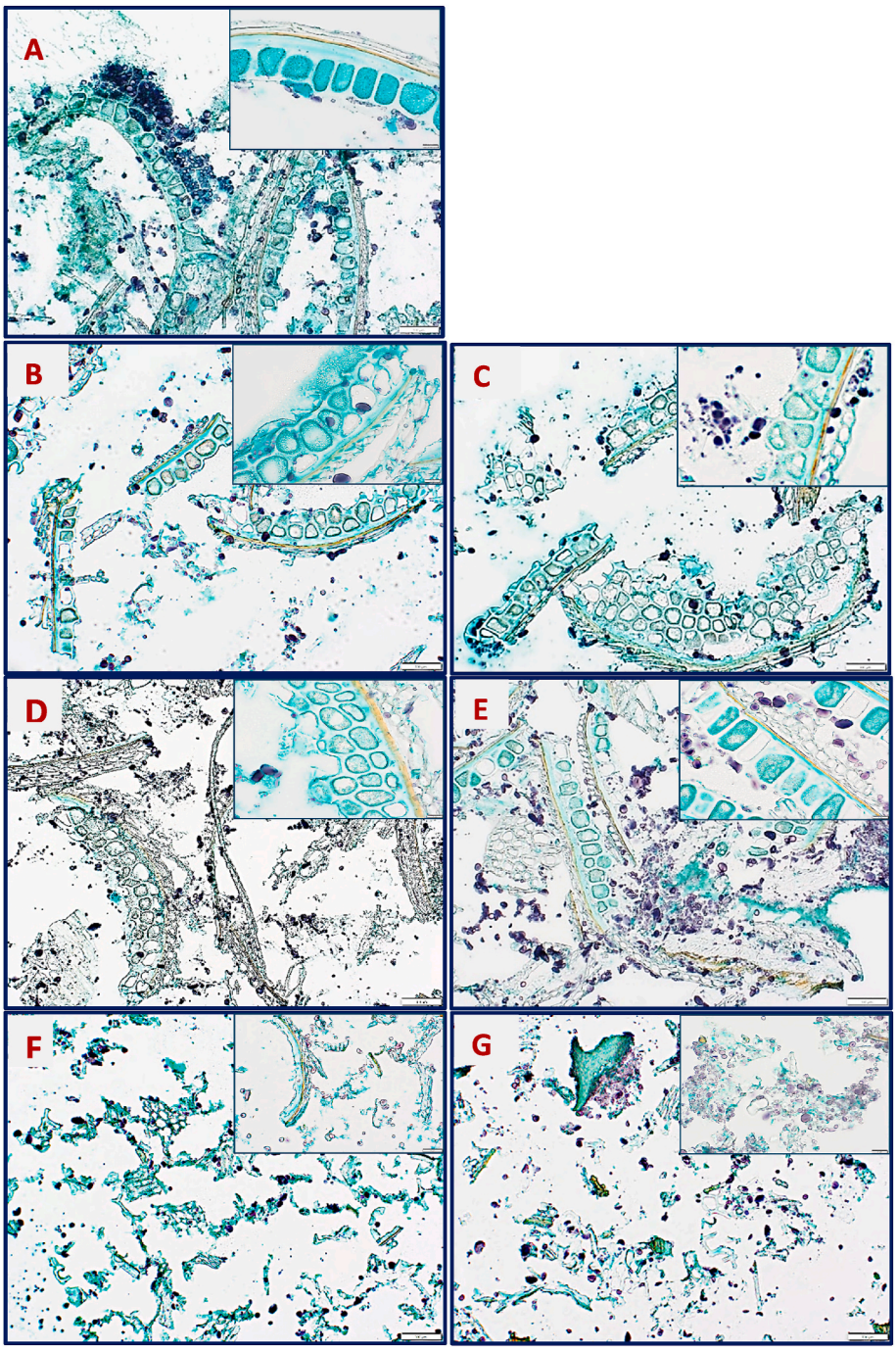

Fig. 1. Microstructures of the starting wheat bran biomass, the homogenate and the first pellet (P1) formed during the pH-shift processing of wheat bran subjected to industrial mill (IM) and its combination with high shear mechanical homogenization for 10 min (10min HSMH) and supermass colloider (SC) at two different magnifications (100 μm) and smaller scale (20 or 50 μm). Proteins are stained green and starch stained blue, but the fibers are unstained. A. Start wheat bran biomass, B. IM Homogenate, C. IM P1, D. 10 min HSMH Homogenate, E. 10 min HSMH P1, F. SC Homogenate, G. SC P1. (For interpretation of the references to color in this figure legend, the reader is referred to the Web version of this article.)

2.6.8. Statistical analysis

Results were reported as mean ± standard deviation (STDEV). Statistical analysis was performed using SPSS Statistics software (version 29.0.1.1; IBM, New York, NY, USA). One-way analysis of variance (ANOVA) was used to determine significant differences between sample groups ($p < 0.05$). Post-hoc comparisons were conducted using Tukey's comparison procedure to verify significant differences between mean values of the analyzed variables.

3. Results and discussion

3.1. Effect of WB milling intensity on protein recovery, mass yield and protein purity

Several milling techniques and intensities were tested as pre-treatments before the pH-shift process to determine which resulted in the highest protein recovery, mass yield, and protein purity (Table 1). The control, which had only experienced industrial milling (IM), showed the lowest protein recovery (29.3 %) and purity (46.1 %) among all

samples. This again proves the difficulty of protein extraction for WB using the pH-shift method, even after mild milling, since most of the proteins are still packed into the aleurone cells surrounded by thick cell walls, as seen in Fig. 1A. Previous research by Alzuwaid et al. (2020) used the pH-shift method to extract proteins from durum wheat bran, employing an alkaline pH of 9.5 for solubilization and a pH of 4.2 for protein precipitation. They achieved 61 % protein purity and a recovery of 20.5–24.8 %. Compared to the current study, their protein purity was slightly higher, while recovery was considerably lower. The lower recovery can be attributed to the milder pH conditions they used, which likely hindered the optimal solubilization of wheat bran proteins. The higher purity despite milder conditions could be explained by their use of a nitrogen-protein conversion factor of 5.7, compared to the 5.4 used in this study. De Brier et al. (2015) investigated the effect of increasing the pH of WB on protein extraction yield also investigated the effect of increasing the pH of wheat bran on protein extraction yield, finding that a pH of 12 resulted in a yield of 37 %, which is still lower than most results from the current study.

Wet milling with HSMH was tested for 3 and 10 min. Longer milling time resulted in higher protein recovery (42 %) and purity (57 %), likely due to the more effective breakdown of the bran structure and increasing accessibility of WB proteins for extraction especially those packed in the aleurone cells which have the highest protein concentration (Brouns et al., 2012). This is in line with the microstructural changes in the WB after HSMH (see Fig. 1D and E) where a larger fraction of aleurone cells where either destroyed or emptied. Dry milling with a ball mill (BM) was tested in three conditions, resulting in protein recovery considerably lower (34–37 %) than those from 10 min HSMH. A combination of wet and dry milling was also tested, using both 3 and 10 min HSMH as well as small, medium, and large BM. However, it did not result any significant improvement in protein recovery compared with HSMH by alone which could mean that the milling efficiency in during HSMH was not improved by using BM WB as the start material or the intensified milling and the degradation did not improve protein extractability during the pH-shift method. Finally, wet milling using a SC resulted in significantly higher protein recovery (42 %) and mass yield (11 %) than the IM but almost equal to 10 min HSMH. Considering the results from microstructure of the WB treated with SC, these findings show that opening aleurone per se and increasing the accessibility to the proteins by alone cannot increase their extractability using the pH-shift method as further discussed in the next part.

3.2. *Microstructure of wheat bran particles*

The effect of extra milling of the industrially milled WB with 10 min-HSMH and SC on its particle size reduction, aleurone structures and release of their protein during the alkaline extraction step of the pH-shift process was visualized with a light microscope (LM) (Fig. 1). The WB start biomass consisted of large particles, with clearly observable intact aleurone cells which were bound to the other layers of the WB (Fig. 1, A). Protein pockets are also visible inside the aleurone cells but also bound to the starchy endosperm, which is in line with what was previously reported for WB structure (Arte et al., 2016; De Bondt et al., 2020). After the addition of water and increasing the pH in the homogenate of the industrially milled sample, proteins outside the aleurone, the starchy endosperm and the proteins inside of some aleurone cells were solubilized in the dispersion (Fig. 1, B) which were partially recovered after the centrifugation as seen in the microstructure of the pellet (Figure, 1, C). By comparing P1 with the start biomass, it is clearly visible in the P1 sample that a part of the aleurone cells have been released while the WB structure is still intact and consists of testa, aleurone and sub-aleurone layers without the aleurone cells (Fig. 1, C). This explains the relatively small protein recovery obtained for the IM sample. The release of protein from aleurone cells, despite their apparently intact walls, could be due to their opening from other dimensions (Fig. 1).

The WB samples subjected to wet milling via 10 min HSMH looked more de-structured and had smaller particles, but most of the aleurone cells were still intact in both homogenate and pellet 1 (Fig. 1D and E). This indicates that 10 min of HSMH treatment was not sufficient to reduce the overall particle size below the dimensions of the aleurone cells, but it effectively opened a larger number of these cells without excessively breaking down other fiber-rich components of the wheat bran. In the homogenate of the wheat bran sample treated with 10 min HSMH, more aleurone cells appeared empty, whereas the P1 sample contained more starch (Fig. 1, D).

Finally, the WB sample treated with SC showed a substantially smaller particle size (20–50 μm) than all the other samples and the WB was completely destructured where almost no aleurone cells could be found (Fig. 1F and G). Protein clusters, starch, and disrupted pieces of histological cell layers such as the testa, pericarp aleurone and hyaline layer are clearly observed in the homogenate of WB sample treated with SC, and a similar story exists for the first pellet of this sample but with a lot less amount of proteins and higher content of starch. This finding is comparable to research conducted by De Bondt et al. (2020) who showed a full dissociation of the bran layers, the AL, and the pericarp layers after grinding WB with a wet bead mill (De Bondt et al., 2020). Dry milling, cryogenic ball milling and impact milling have also proven to be successful in releasing the AL from the WB cell layers and breaking down the WB structure (De Bondt et al., 2020; Hemery, Chaurand, et al., 2011). Overall, more proteins are found in the homogenates than in the P1 samples and the P1 samples were richer in starch. This is in line with the improvements in the protein recovery and purity obtained by applying SC to the samples compared with the control (Table 1). However, not achieving a higher protein recovery despite the very effective milling and opening of the aleurones using SC compared with 10 MHSMH is in contrast with our expectations and what was previously reported for improvement of protein solubility and digestibility by

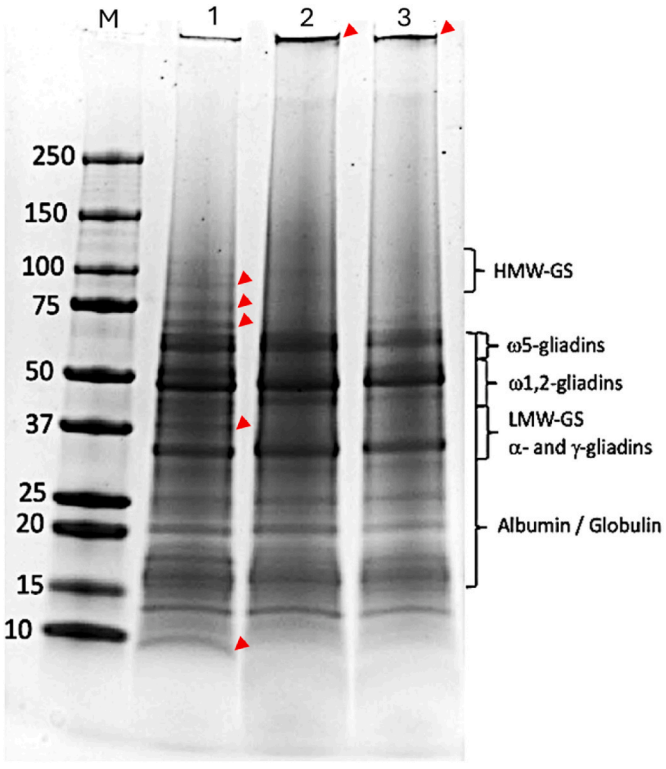

Fig. 2. Gel-electrophoresis of protein recovered from wheat bran (WB) subjected to industrial milling (IM) and its combination with high-shear mechanical homogenization for 10 min (10min HSMH) and supermass colloider (SC). M: Marker, 1: protein from WB IM, 2: Protein from WB 10 min HSMH, 3: protein from WB SC, LMW-GS: Low-molecular weight glutelin's, HMW: High-molecular weight glutelin's.

milling down to a size below the aleurone dimensions (Li et al., 2023). This might be due to the breakdown and release of other components, especially fibers which could have reduced protein precipitation in the second step of the pH-shift process. This is in line with a much lower content of starch and fibers observed in the 1st pellet of the sample treated with SC compared with the one treated with HSMH. In addition, it could mean that the released proteins by other aleurones are tightly bound to the fibers which are anyhow not extractable or recoverable using the classic pH-shift method. Overall, results showed that fine milling of WB and opening of the aleurone cells can result in better access for the extraction of proteins but cannot guarantee their recovery using the pH-shift technology.

3.3. Effect of fine milling on the properties of recovered WB proteins

3.3.1. Polypeptide pattern of proteins

The electrophoretic polypeptide patterns of recovered protein concentrate from WB subjected to different milling can be seen in Fig. 2. The polypeptide pattern of the recovered WB proteins had similarities to what had previously been reported for proteins in WB and wheat flour (De Brier et al., 2015; Schalk et al., 2017). All three recovered proteins were abundant in ω1,2-gliadins (43–60 kDa), ω5-gliadins (60–68 kDa), α- and γ-gliadins, low-molecular-weight glutelin subunits (LMW-GS) (32–45 kDa) and albumin and especially globulin (14–60 kDa) (De Brier et al., 2015). This suggests a successful extraction of aleurone albumin and globulin proteins which is in line with the changes observed in the LM micrographs (Fig. 1). The 7 S globulins in wheat are the major storage protein in aleurone cells but are not present in starchy endosperm cells (Khan, 2009). At the same time, it remains challenging to identify the proteins sizing 32–60 kDa since those may derive from aleurone or endosperm glutelin's, endosperm gliadins or from albumin/globulin fraction of the aleurone (De Brier et al., 2015). Moreover, previous research on WB found that the MW distribution of the prolamin and gliadin fractions had large similarities (De Brier et al., 2015; Schalk et al., 2017). Peaks between 30 and 43 kDa were associated with α-type and γ-type gliadin and a broad peak around 66 k to ω-type gliadin. Thus, it was concluded that the prolamin fraction most likely consists of gliadin from endosperm contamination in the bran (cf. supra and infra).

The amount of high-molecular-weight bands associated with glutelin subunits (HMW-GS), decreased within the proteins recovered from WB subjected to harsher milling with both HSMH and SC. The difference can be observed by the noticeable bands for proteins recovered from IM WB with MW between 60 and 110 kDa that were not visible for the other two samples. Overall, a larger number of bands with more intensity were seen for the protein from IM both in the MW range of the known polypeptides around 37 kDa, and for smaller peptides below approx. 14 kDa.

Another main finding is that the particle size reduction using 10 min HSMH and SC resulted in bands appearing at the top of the stacked gel, at >250 kDa. This can potentially be due to the aggregation of proteins during harsh milling or related to the HMW proteins formed during the 10 min HSMH and SC processes. Those proteins might not have been extracted from the IM biomass, but extracted for the other two milling processes due to crosslinking of proteins or the release of HMW proteins together with other compounds such as phenolic compounds (Li and Lee, 1998). Overall, the results showed that the type and intensity of milling can affect the polypeptide pattern of WB protein recovered using the pH-shift method, where harsher milling results in lower detectable content of glutelin subunits. De Brier et al. (2015) previously reported that aleurone contains mostly globulin and albumin but WB might be contaminated with a substantial amount of glutelin from endosperm which could be extracted using Osborn method after ball milling (De Brier et al., 2015). However, recovering those proteins using the pH-shift method after opening AL using SC was not possible.

3.3.2. Zeta potential and particle size of proteins

Zeta potential (ζ) characterizes the surface charge of a protein, which is often a balance of non-polar hydrophobic residues, hydrophilic polar groups (-OH and -NH_2), and ionic groups (-NH_3^+ and -COO^-) generated through the ionization of surface amino acids (Ge et al., 2021). The zeta potential indicates the colloidal stability of a protein solution: values close to ±0–10 mV indicate high instability, ±10–20 mV indicate relative stability, ±20–30 mV indicate moderate stability, and values greater than ±30 mV indicate high stability. This classification is commonly used in drug delivery literature (Bhattacharjee, 2016).

The zeta potential of the three WB proteins was highest at acidic and alkaline conditions (pH 3 and 11), and lowest at or near the isoelectric point (around pH 5) (Fig. 3, B). These findings are consistent with previous studies on wheat and other plant-based proteins (Rani et al., 2023). When the surface hydrophobicity rises, an increase in protein insolubility and aggregation occurs which leads to a decrease in zeta potential (Rani et al., 2023). All samples showed their minimum zeta potential values around pH 5.0, where the zeta potential was near zero. The biggest difference between the samples was observed at pH 9.0: protein from the industrial mill and 10 min HSMH exhibited the most negative zeta potential, while SC protein had a less negative value by

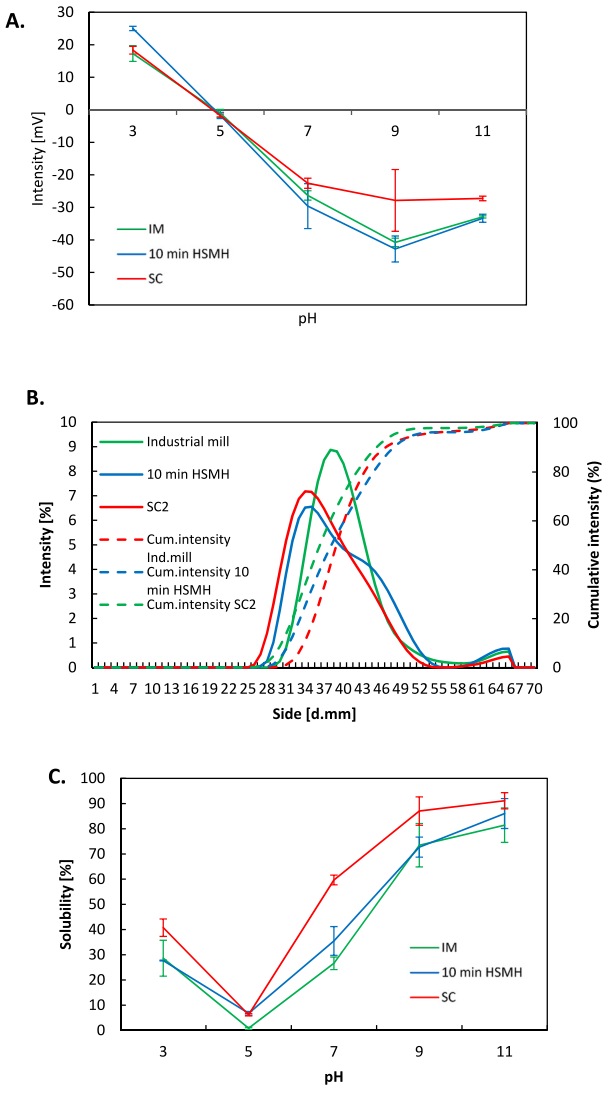

Fig. 3. Zeta potential as a function of pH (A), particle size distribution at pH 7 (B) and water solubility as a function of pH (C) of proteins recovered from wheat bran subjected to industrial milling (IM) and its combination with high shear mechanical homogenization for 10 min (10min HSMH) and suppermass colloider (SC).

approximately 15 mV. This can be explained by SC protein being the most finely ground sample, resulting in the smallest particle size, which enhances protein-water interaction and contributes to greater colloidal stability at alkaline pH (Rani et al., 2023). This is due to the ionization of partially buried sulfhydryl, carboxylic, phenolic, and tyrosine residues within the protein structure. These residues contribute to an increase in the overall net charge of the protein molecules, leading to a stronger intramolecular electrostatic repulsion. Consequently, this prompts greater swelling and unfolding of the proteins, which therefore bind to more water molecules (Damodaran, 2017). This is applicable at the positive intensity of the zeta potential where the most grinded sample, SC, had the highest intensity, then the 10 min HSMH and finally the least grinded sample, IM. However, the results are contradictory at the negative intensity, where the SC is least negative, and the 10 min HSMH and IM samples are more negative and similar.

The particle size distribution of proteins recovered from wheat bran using three different milling techniques also revealed distinct variations in intensity and cumulative intensity profiles (Fig. 3B). The IM method resulted in proteins with a broad distribution with a prominent peak at larger particle sizes, indicating a coarser product. In contrast, the 10-min HSMH treatment led to a significant ($p < 0.05$) reduction in particle size, as evidenced by a shift towards smaller particle sizes in the distribution, resulting in higher intensity at lower diameters. This suggests that HSMH effectively disrupted the bran structure, leading to finer protein particles. The SC2 milling method displayed the most pronounced shift towards smaller particles, achieving the lowest average particle size and the highest overall intensity at lower diameters, which could enhance protein solubility and functional properties.

The cumulative intensity curves indicate that the SC treatment also resulted in a more uniform distribution of smaller particles, which may contribute to improved extraction efficiency and potential functionality of the recovered proteins (Zhao et al., 2020).

3.3.3. Protein solubility in water

The solubility of the WB protein concentrates in water was analyzed at different pH values (Fig. 3, C). The lowest protein solubility of 0.8–6.8 % was observed at pH 5.0, representing the pI of the proteins due to the reduction in electrostatic repulsion, where the samples also showed a zeta potential of zero (Fig A). This is in line with a previously reported isoelectric point for wheat bran proteins of 4.5–5 (Alzuwaid et al., 2020). The protein solubility increased at the most acidic condition of pH 3.0 for all samples. A sharp initial increase was obtained when increasing the pH from pH 5.0 up to pH 7.0 and 9.0, followed by a smaller increase between pH 9.0 and 11.0. Protein solubility between 81.4 and 91.1 % was seen at pH 11.0 for the samples. The high solubility of the WB protein samples at alkaline conditions is explained by the fact that the most abundant proteins in all the samples were albumin and globulin, based on the SDS-PAGE results (Fig. 3), which are water or alkaline-soluble proteins. Similar results have been previously reported for solubility of WB proteins vs pH (Arte et al., 2019; De Brier et al., 2015). The protein produced from WB treated with SC had the highest water solubility of all samples at the entire pH range. This could be related to the higher percentage of globulin and albumin in SC protein compared with the industrial mill protein which contained glutelin fractions that are mostly alcohol soluble (Fig. 3). The higher water solubility of SC protein could be also related to its smaller particle size (Fig. 3, B). This could be the effect of harsh milling with SC which has broken down protein aggregates into smaller particles which normally results in better water solubility with lower protein particle size (Zhao et al., 2020). Previous studies on other plant-based resources e.g. soy and faba bean, have also shown that lower particle size results in higher water solubility (Yang et al., 2018; Zhao et al., 2020). It is worth noting that a higher protein water solubility is highly desirable since low protein solubility has been shown to adversely affect their functional properties, thereby diminishing their effectiveness in various food applications (Alzuwaid et al., 2020).

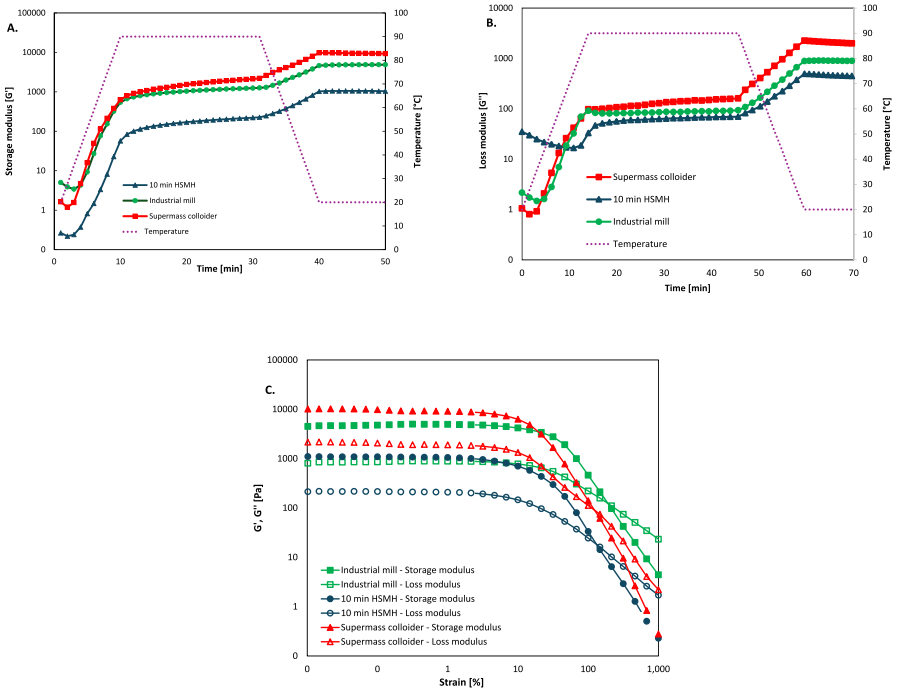

Fig. 4. Rheological behaviors (storage modulus G' (A.) and loss modulus G'' (B) over time) of protein gels made of protein from wheat bran (WB) subjected to industrial milling (IM) and its combination with high shear mechanical homogenization for 10 min (10min HSMH) and supermass colloider (SC) during in situ gelation via temperature ramp test including an initial heating step (5 °C/min, from 20 to 90 °C), followed by an isothermal step (90 °C, 30 min) and a final cooling step (5 °C/min, from 90 to 20 °C) and (C) results for amplitude sweep of the gels at the end of gelation process, showing the limit of the linear viscoelastic (LVE) region and the flow points at the crossover points (G' = G″) for each sample.

3.3.4. Rheological properties of the protein concentrates

The changes in rheological properties of proteins from WB at different temperatures over time are shown in Fig. 4. The storage modulus represents material's ability to store energy, called the elastic portion, whereas the loss modulus represents material's ability to dissipate energy as heat, called the viscous portion. As expected, the gelation process started with a reduction in G′ for all proteins due to protein denaturation (Fig. 4A and B). A sharp increase in G′ was found between 5 and 11 min (i.e., 20–60 °C) reflecting a structure formation of proteins. During the 30 min period at 90 °C, a slight increase in G′ was obtained for the protein from 10 min HSMH and SC, indicating a good structure formation, whereas the protein from IM WB remained stable. The protein from SC WB had the highest G′ during and at the end of the *in-situ* gelation process, representing a better structure formation than the others. Similar trends were noticed for the loss modulus, G″, for all the proteins from WB, showing improvement in the viscoelasticity of the samples overheating. The better gel-forming ability of the protein recovered with the aid of SC compared with the IM protein could be related to its higher purity, smaller particle size and better water solubility. Proteins with smaller particle sizes and higher water solubility have enhanced gel formation capacity due to improved hydration, dispersion, and increased surface area, which promote stronger protein-protein and protein-water interactions (Khan, 2009). The lower gel-forming ability of HSMH protein compared with IM, despite its higher purity could be related to the higher proportion of lower molecular weight proteins, which may have reduced its gel-forming capacity. This is because lower molecular weight proteins have fewer opportunities to form the extensive cross-links and intermolecular interactions needed to create a stable gel network, resulting in a weaker gel structure (van der Linden and Foegeding, 2009; Khan, 2009). However, it is important to consider that all the recovered protein concentrates contained other components that might have contributed to the observed rheological properties and the differences.

The textural properties of the protein gels from WB were tested using a small-amplitude oscillation test, called the amplitude sweep test (Fig. 4C). At intermediate strains (~5 %) the WB protein gels showed higher G′ than G″ in the range of strain amplitude, suggesting that they predominantly behaved as a soft elastic material. As the strain exceeded 5 %, the G′ curve decreased and eventually crossed the G″ curve, suggesting a viscous response and a structure breakdown of the WB protein gels. The gap between the G′ and G″ was different for each sample at intermediate strains (below 5 %). The protein from WB subjected to 10 min HSMH had the smallest gap (~800 Pa) and is therefore less viscoelastic than the other two samples. The yield stress was determined by the crossover point of G′ and G″ for each sample. The protein from WB treated 10 min HSMH and SC had very similar yield stress. However, the protein from WB treated only with the IM had a slightly higher crossover point (by a margin of 55–77 % for strain) and is therefore a stronger gel (Fig. 4C, line with squares). This means that the gel made of SC protein was relatively stiff in its elastic region, meaning it can store more energy and resist deformation under small strains. However, its lower yield stress implies that it is easier to break down or flow once a certain stress

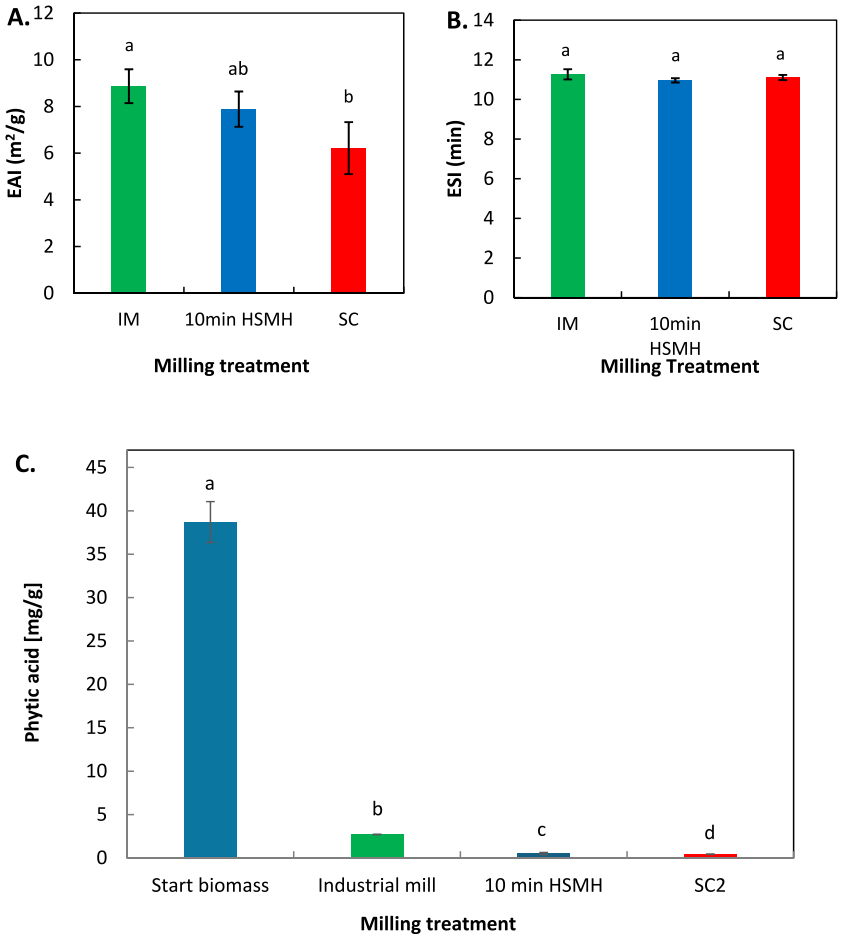

Fig. 5. Emulsion activity index (EAI (A), emulsion stability index (ESI) (B) and phytic acid content (C) of proteins recovered from wheat bran subjected to industrial milling (IM), its combination with high shear mechanical homogenization for 10 min (10min HSMH) and suppermass colloider (SC). Different small letters define significant differences between the sample's EAI and ESI mean values ($p < 0.05$).

threshold is reached. This could be due to the higher proportion of low molecular weight proteins in both SC and HSMH proteins compared with the IM proteins. A protein with a lower molecular weight may form a stiffer gel network initially (higher G′) due to tight packing or dense intermolecular interactions. However, because of the shorter chains and fewer cross-linking opportunities, the network can be disrupted more easily, leading to a lower yield stress (van der Linden and Foegeding, 2009).

3.3.5. Emulsion capacity of the wheat bran proteins

Emulsifying capacity refers to the ability of emulsifying agents to create a layer at the oil water, ensuring the stability of the emulsion (Xu et al., 2018). Results showed that protein from IM had the highest EAI and ESI while protein from WB subjected to SC showed the lowest EAI ($p < 0.05$) (Fig. 5A and B). However, results were statistically insignificant between ESI for the samples. The EAI of the protein from WB was reduced from 8.87 to 6.21 m^2/g by using 10 min HSMH and SC, but the emulsifying stability did not change much. The decrease in EAI without a decrease in ESI shows the lack of relation between the two functional properties. Contradictory results between EAI and ESI were also reported by Liu et al. (2021) where EAI improved with increased ball milling time, whereas ESI initially decreased but then increased by extended ball milling and reduced particle size. The lower EAI of the protein from SC could be related to its lower zeta potential (see Fig. 3A), indicating reduced electrostatic repulsion between protein particles, which can lead to aggregation rather than forming stable emulsions. It could also be related to their lower particle size and polypeptide pattern. Lower molecular weight proteins often exhibit reduced charge density, leading to lower zeta potential and weaker electrostatic repulsion between droplets, which can hinder the initial emulsion formation process (Lam and Nickerson, 2013).

3.3.6. Phytic acid content

The phytic acid content of white wheat flour is generally in the range of 1.3–4.5 mg/g, but it is up-concentrated to a high level in WB and has been measured around 42–97 mg/g (Wu et al., 2010). Here, the phytate content of the start WB biomass was found to be 38.71 mg/g (Fig. 5 C). Regardless of the applied milling method, the protein extraction process per se resulted in a substantial reduction of phytate, resulting in a very small residue of phytate in all the recovered proteins. This is most probably due to the dissociation of phytate from protein and their precipitation at the alkaline conditions used to extract WB proteins, which effectively happen at pH values 10–11.5 (Wang and Guo, 2021). The content of phytate in the proteins recovered from the WB subjected to IM, 10 min HSMH and SC was reduced to 2.70, 0.52 and 0.42 mg/g. As can be seen, further reduction of WB particle size with the aid of HSMH and SC resulted in even more effective removal of phytate during the pH-shift method, resulting in the lowest amount of phytate in the protein from WB milled with SC. This reduction was explained by the fact that larger particle sizes of WB are obtained from outer bran layers and hence contain a higher phytic acid content than the inner layers which are smaller in particle size. It is also claimed that the reduction in phytic acid can be attributed to the particle size on the extractability of phytate which was made easier when the particle size was reduced (Chen et al., 2013). In our study, since the aleurone cells were destroyed after milling with SC, we could expect that more phytate would be released into the protein extraction medium. However, it seems that since the phytate was not coextracted with the protein and rather more efficiently removed by destroying the aleurone cells as its main reservoir. Extensive milling reduces the particle size of wheat bran, increasing the surface area available for interactions and more effective access to phytate molecules during the extraction process, facilitating their solubilization and removal. Recently, Chuchuca Moran and Grossmann (2025) also reported that increasing milling energy during the milling of pea seeds improves the removal of phytate from pea protein during its extraction using the pH-shift method (Chuchuca Moran and Grossmann, 2025).

3.3.7. Colorimetry

The color of WB proteins can be mostly related to their content of anthocyanins and carotenoids. Anthocyanin compounds are mainly located in the bran and particularly in the AL of cereal grains, whereas the carotenoids provide the yellow pigmentation of the endosperm (Meziani et al., 2021). The color of the proteins recovered from the WB was influenced by the type of milling used for their production, where WB protein treated with IM was lighter in color than WB protein subjected to 10 min HSMH and SC (Fig. 6 and Table 2). Liu et al. (2021) found that size reduction using ball milling significantly increased wheat gluten proteins' whiteness. However, in our study, more milling and particle size reduction resulted in increased darkness of the WB protein. It is therefore hypothesized that the dark color that is seen after the harsh milling could be attributed to the release of anthocyanin compounds from AL which could have been co-extracted with the proteins or due to upconcentration of other phenolic compounds which can induce darkening when oxidized during the pH-shift processing as reported for other proteins such as rapeseed, sunflower seed or faba beans (Yang

Table 2
Surface Color parameters of proteins recovered from WB subjected to industrial milling, 10 min high shear mechanical homogenization (10 min HSMH) and supermass colloider (SC).

	Industrial mill	10 min HSMH	Supermass colloider
L	57.67 ± 0.14^{b}	62.39 ± 0.08^{a}	54.24 ± 0.06^{c}
a	4.54 ± 0.04^{a}	4.15 ± 0.04^{b}	2.88 ± 0.015^{c}
b	12.32 ± 0.03^{b}	15.25 ± 04^{a}	8.73 ± 0.01^{c}

Different small letters in each row show statistical significant differences ($p < 0.05$).

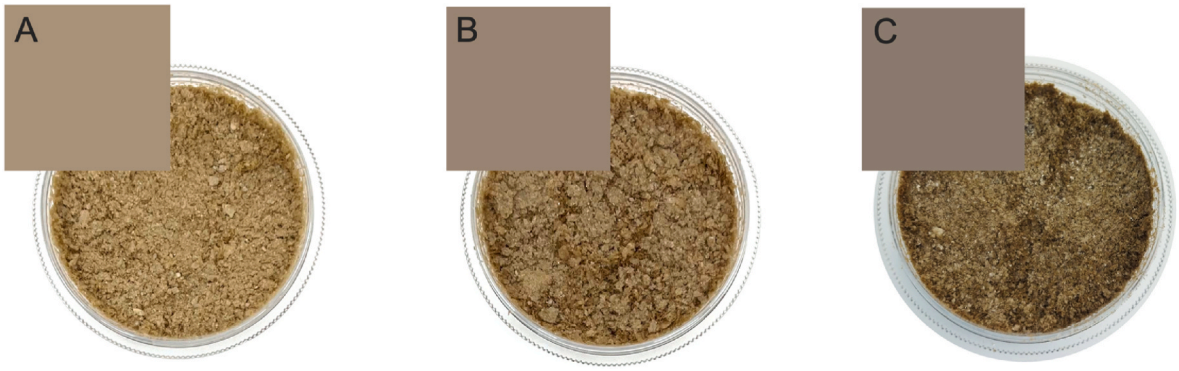

Fig. 6. Representative picture of proteins recovered from WB subjected to industrial milling (A) and 10 min high shear mechanical homogenization (10 min HSMH) (B) and supermass colloider (SC) (C).

et al., 2018).

4. Conclusions

Various wet- and dry-milling techniques were investigated to reduce wheat bran (WB) particle size, aiming to destructure it down to aleurone cells and facilitate protein recovery using the pH-shift method. Wet milling with both HSMH and SC increased protein recovery and purity by approximately 12 % and 10 %, respectively. Complete destructuring of WB to aleurone cells was achieved only with SC; however, this did not result in higher protein recovery, likely due to the strong binding of released proteins to fibers and other WB components, which hindered their extraction despite improved accessibility. The effects of fine milling extended beyond protein recovery and purity. Both HSMH and SC led to substantially smaller particle size distributions and lower molecular weight distributions in the recovered WB proteins. SC, in particular, significantly improved water solubility (more than 2-fold at pH 7) and gel-forming capacity of WB protein, although it reduced emulsification activity and whiteness compared with IM. Phytate was effectively removed during protein recovery, with fine milling by HSMH and SC increasing its removal 5- and 6-fold compared to IM. Considering the functionality results, it seems that WB protein could have potential for application as a gel-forming agent but further studies are necessary to verify its functionality in gel-based systems. Overall, this study demonstrates the potential of optimizing the milling step to enhance protein recovery from WB while also providing a novel approach for engineering protein functionality. Future research should focus on optimizing the pH-shift method to recover proteins released by the opening of aleurone cells and also comparing the functionality and values proposed with the recovered WB protein with WB flour and wheat flour protein.

CRediT authorship contribution statement

Helga Gudny Eliasdottir: Writing – original draft, Visualization, Methodology, Investigation, Formal analysis, Data curation. **Precious Elue Ebube:** Methodology, Investigation, Formal analysis. **Annika Krona:** Methodology, Formal analysis, Data curation. **E.R. Kanishka B. Wijayarathna:** Methodology, Investigation. **Akram Zamani:** Writing – review & editing, Resources. **Mehdi Abdollahi:** Writing – review & editing, Visualization, Resources, Project administration, Funding acquisition, Conceptualization.

Declaration of competing interest

The authors declare that they have no known competing financial interests or personal relationships that could have appeared to influence the work reported in this paper.

Acknowledgments

We are grateful to FORMAS for the research grant within the 3DMix project (grant number: 2021-02349). We are also thankful to Lantmännen for all their contribution to the study not the least the samples and industrial reflections. We are grateful to Miakela Isabel Badager and Elahe Sharifi for their help during the analysis.

Data availability

Data will be made available on request.

References

Alzuwaid, N.T., Sissons, M., Laddomada, B., Fellows, C.M., 2020. Nutritional and functional properties of durum wheat bran protein concentrate. Cereal Chem. 97, 304–315. https://doi.org/10.1002/cche.10246.

Arte, E., Huang, X., Nordlund, E., Katina, K., 2019. Biochemical characterization and technofunctional properties of bioprocessed wheat bran protein isolates. Food Chem. 289, 103–111. https://doi.org/10.1016/j.foodchem.2019.03.020.

Arte, E., Katina, K., Holopainen-Mantila, U., Nordlund, E., 2016. Effect of hydrolyzing enzymes on wheat bran cell wall integrity and protein solubility. Cereal Chem. 93, 162–171. https://doi.org/10.1094/CCHEM-03-15-0060-R.

Bhattacharjee, S., 2016. DLS and zeta potential - what they are and what they are not? J. Contr. Release 235, 337–351. https://doi.org/10.1016/j.jconrel.2016.06.017.

Brouns, F., Hemery, Y., Price, R., Anson, N.M., 2012. Wheat aleurone: separation, composition, health aspects, and potential food use. Crit. Rev. Food Sci. Nutr. 52, 553–568. https://doi.org/10.1080/10408398.2011.589540.

Carlsson, N.G., Bergman, E.L., Skoglund, E., Hasselblad, K., Sandberg, A.S., 2001. Rapid analysis of inositol phosphates. J. Agric. Food Chem. 49, 1695–1701. https://doi.org/10.1021/jf000861r.

Chen, Z., Mense, A.L., Brewer, L.R., Shi, Y.C., 2023. Wheat bran layers: composition, structure, fractionation, and potential uses in foods. Crit. Rev. Food Sci. Nutr. 1–24. https://doi.org/10.1080/10408398.2023.2171962, 0.

Chen, Zhongwei, Zha, B., Wang, L., Wang, R., Chen, Zhengxing, Tian, Y., 2013. Dissociation of aleurone cell cluster from wheat bran by centrifugal impact milling. Food Res. Int. 54, 63–71. https://doi.org/10.1016/j.foodres.2013.05.032.

Chuchuca Moran, G., Grossmann, L., 2025. Milling energy impacts the co-extraction of globulins, albumins, and anti-nutritional factors of peas. Food Bioprocess Technol. 18 (2), 1534–1548.

Damodaran, S., 2017. Fennema's Food Chemistry, fifth ed. CRC Press. https://doi.org/10.1201/9781315372914.

De Bondt, Y., Liberloo, I., Roye, C., Windhab, E.J., Lamothe, L., King, R., Courtin, C.M., 2020. The effect of wet milling and cryogenic milling on the structure and physicochemical properties of wheat bran. Foods 9, 1–16. https://doi.org/10.3390/foods9121755.

De Brier, N., Gomand, S.V., Celus, I., Courtin, C.M., Brijs, K., Delcour, J.A., 2015. Extractability and chromatographic characterization of wheat (*Triticum aestivum* L.) bran protein. J. Food Sci. 80, C967–C974. https://doi.org/10.1111/1750-3841.12856.

Ge, J., Sun, C.X., Mata, A., Corke, H., Gan, R.Y., Fang, Y., 2021. Physicochemical and pH-dependent functional properties of proteins isolated from eight traditional Chinese beans. Food Hydrocoll. 112, 106288. https://doi.org/10.1016/j.foodhyd.2020.106288.

Guo, J., Bian, Y.Y., Zhu, K.X., Guo, X.N., Peng, W., Zhou, H.M., 2015. Reducing phytate content in wheat bran by directly removing the aleurone cell content with teeth roller mill and ultrasonic cleaner. J. Cereal. Sci. 64, 133–138. https://doi.org/10.1016/j.jcs.2015.03.012.

Hemery, Y., Chaurand, M., Holopainen, U., Lampi, A.M., Lehtinen, P., Piironen, V., Sadoudi, A., Rouau, X., 2011. Potential of dry fractionation of wheat bran for the development of food ingredients, part I: influence of ultra-fine grinding. J. Cereal. Sci. 53, 1–8. https://doi.org/10.1016/j.jcs.2010.09.005.

Janssen, F., Courtin, C.M., Wouters, A.G.B., 2023. Aqueous phase extractable protein of wheat bran and germ for the production of liquid and semi-solid foods. Crit. Rev. Food Sci. Nutr. 1–19. https://doi.org/10.1080/10408398.2023.2214615, 0.

Khan, K., 2009. Review of Wheat: Chemistry and Technology, fourth ed. Woodhead Publishing and AACC International Press. https://doi.org/10.1080/10496500903245487.

Li, C., McClements, D.J., Dai, T., Deng, L., Feng, Z., Li, T., Liu, C., Chen, J., 2023. Enhancing the dispersibility of commercial pea protein ingredients using stirred media milling: potential mechanisms of action. Food Hydrocoll. 145, 109130. https://doi.org/10.1016/j.foodhyd.2023.109130.

Laemmli, U.K., 1970. Cleavage of structural proteins during the assembly of the head of bacteriophage T4. Nature 227, 680–685.

Lam, R.S.H, Nickerson, M.T., 2013. Food proteins: A review on their emulsifying properties using a structure–function approach. Food Chem. 141 (2), 975–984.

Li, Mei, Lee, Tung-Ching, 1998. Effect of cysteine on the molecular weight distribution and the disulfide cross-link of wheat flour proteins in extrudates. J. Agric. Food Chem. 46 (3), 846–853.

Li, Y., Wang, H., Wang, Lijuan, Qiu, J., Li, Z., Wang, Lili, 2023. Milling of wheat bran: influence on digestibility, hydrolysis and nutritional properties of bran protein during in vitro digestion. Food Chem. 404, 134559. https://doi.org/10.1016/j.foodchem.2022.134559.

Liu, Z., Zheng, Z., Zhu, G., Luo, S., Zhang, D., Liu, F., Shen, Y., 2021. Modification of the structural and functional properties of wheat gluten protein using a planetary ball mill. Food Chem. 363, 130251. https://doi.org/10.1016/J.FOODCHEM.2021.130251.

Mariotti, F., Tomé, D., Mirand, P., 2019. Converting nitrogen into protein – beyond 6.25 and jones ' factors. Crit. Rev. Food Sci. Nutr. 48, 1–21.

Markwell, M.A.K., Haas, S.M., Bieber, L.L., Tolbert, N.E., 1978. A modification of the Lowry procedure to simplify protein determination in membrane and lipoprotein samples. Anal. Biochem. 87, 206–210.

Meziani, S., Nadaud, I., Tasleem-Tahir, A., Nurit, E., Benguella, R., Branlard, G., 2021. Wheat aleurone layer: a site enriched with nutrients and bioactive molecules with potential nutritional opportunities for breeding. J. Cereal. Sci. 100, 103225. https://doi.org/10.1016/j.jcs.2021.103225.

Onipe, O.O., Beswa, D., Jideani, A.I.O., 2017. Effect of size reduction on colour, hydration and rheological properties of wheat bran. Food Sci. Technol. 37, 389–396. https://doi.org/10.1590/1678-457x.12216.

Oreopoulou, V., Tzia, C., 2007. Utilization of plant by-products for the recovery of proteins, dietary fibers, antioxidants, and colorants. Utilization of By-Products and Treatment of Waste in the Food Industry, pp. 209–232. https://doi.org/10.1007/978-0-387-35766-9_11.

Rani, M., Siddiqi, R.A., Sharma, R., Gill, B.S., Sogi, D.S., 2023. Functional and structural properties of gliadin as influenced by pH, extraction protocols, and wheat cultivars. Int. J. Biol. Macromol. 234, 123484. https://doi.org/10.1016/j.ijbiomac.2023.123484.

Sajib, M., Forghani, B., Kumar Vate, N., Abdollahi, M., 2023. Combined effects of isolation temperature and pH on functionality and beany flavor of pea protein isolates for meat analogue applications. Food Chem. 412. https://doi.org/10.1016/j.foodchem.2023.135585.

Schalk, K., Lexhaller, B., Koehler, P., Scherf, K.A., 2017. Isolation and characterization of gluten protein types from wheat, rye, barley and oats for use as reference materials. PLoS One 12, 1–20. https://doi.org/10.1371/journal.pone.0172819.

Thakur, Abhishek, Sharma, V., Thakur, Aayushee, Vishal Sharma, C., 2019. An overview of anti-nutritional factors in food. Int. J. Chem. Stud. 7, 2472–2479.

van der Linden, E., Foegeding, E.A., 2009. Gelation: Principles, models and applications to proteins. Modern Biopolymer Science. Academic press, pp. 29–91.

Wang, R., Guo, S., 2021. Phytic acid and its interactions: contributions to protein functionality, food processing, and safety. Compr. Rev. Food Sci. Food Saf. 20, 2081–2105. https://doi.org/10.1111/1541-4337.12714.

Wu, P., Zhao, T., Tian, J.C., 2010. Phytic acid contents of wheat flours from different mill streams. Agric. Sci. China 9, 1684–1688. https://doi.org/10.1016/S1671-2927(09)60266-2.

Xu, Y., Wang, C., Fu, X., Huang, Q., Zhang, B., 2018. Effect of pH and ionic strength on the emulsifying properties of two Octenylsuccinate starches in comparison with gum Arabic. Food Hydrocoll. 76, 96–102. https://doi.org/10.1016/j.foodhyd.2017.02.015.

Yang, J., Liu, G., Zeng, H., Chen, L., 2018. Effects of high pressure homogenization on faba bean protein aggregation in relation to solubility and interfacial properties. Food Hydrocoll. 83, 275–286. https://doi.org/10.1016/j.foodhyd.2018.05.020.

Zhao, X., Sun, L., Zhang, X., Liu, H., Zhu, Y., 2020. Effects of ultrafine grinding time on the functional and flavor properties of soybean protein isolate. Colloids Surf. B Biointerfaces 196. https://doi.org/10.1016/j.colsurfb.2020.111345.